© 2017. Published by The Company of Biologists Ltd | Development (2017) 144, 2082-2091 doi:10.1242/dev.149930

RESEARCH ARTICLE

Sonic hedgehog regulation of *Foxf2* promotes cranial neural crest mesenchyme proliferation and is disrupted in cleft lip morphogenesis

Joshua L. Everson[1,2], Dustin M. Fink[1], Joon Won Yoon[3], Elizabeth J. Leslie[4], Henry W. Kietzman[1], Lydia J. Ansen-Wilson[1], Hannah M. Chung[1,2], David O. Walterhouse[3], Mary L. Marazita[4] and Robert J. Lipinski[1,2,*]

ABSTRACT

Cleft lip is one of the most common human birth defects, yet our understanding of the mechanisms that regulate lip morphogenesis is limited. Here, we show in mice that sonic hedgehog (Shh)-induced proliferation of cranial neural crest cell (cNCC) mesenchyme is required for upper lip closure. Gene expression profiling revealed a subset of Forkhead box (Fox) genes that are regulated by Shh signaling during lip morphogenesis. During cleft pathogenesis, reduced proliferation in the medial nasal process mesenchyme paralleled the domain of reduced *Foxf2* and *Gli1* expression. SHH ligand induction of *Foxf2* expression was dependent upon Shh pathway effectors in cNCCs, while a functional GLI-binding site was identified downstream of *Foxf2*. Consistent with the cellular mechanism demonstrated for cleft lip pathogenesis, we found that either SHH ligand addition or *FOXF2* overexpression is sufficient to induce cNCC proliferation. Finally, analysis of a large multi-ethnic human population with cleft lip identified clusters of single-nucleotide polymorphisms in *FOXF2*. These data suggest that direct targeting of *Foxf2* by Shh signaling drives cNCC mesenchyme proliferation during upper lip morphogenesis, and that disruption of this sequence results in cleft lip.

KEY WORDS: Sonic hedgehog, Orofacial morphogenesis, Cleft lip, Forkhead box, Cranial neural crest cell, Medial nasal process, Human, Mouse

INTRODUCTION

Morphogenesis of the upper lip and palate requires orchestrated growth and fusion of embryonic facial growth centers (Jiang et al., 2006; Lan et al., 2015). Epithelial-mesenchymal cross-talk that drives cellular proliferation and tissue outgrowth is required for closure of both the upper lip and palate. Disruption of these processes results in orofacial clefts (OFCs), which are among the most common human birth defects (Rahimov et al., 2012; Murthy and Bhaskar, 2009). OFCs are genetically complex traits, but racial disparity in prevalence, heightened recurrence rates among siblings, and 50% concordance rates in monozygotic twins indicate an important hereditary component (Lidral et al., 2008). Genome-wide studies have identified multiple associated loci, but our understanding of the genetic underpinnings of OFCs is incomplete, particularly for cases considered non-syndromic (Lidral et al., 2008; Leslie et al., 2013).

Animal models have proven to be powerful for elucidating the mechanisms that drive human birth defects, but the vast majority of mouse OFC models exhibit clefts of the secondary palate with an intact upper lip, whereas most human OFC cases involve clefts of the upper lip (Watkins et al., 2014; Gritli-Linde, 2008, 2012). Consequently, our understanding of the molecular and cellular mechanisms of upper lip development is minimal relative to that of secondary palate morphogenesis.

Experiments in mouse and chick have shown that the sonic hedgehog (Shh) signaling pathway regulates morphogenesis of the tissues that form the midface. Specifically, secretion of SHH ligand from the ectoderm activates pathway activity in the adjacent cranial neural crest-derived mesenchyme (Marcucio et al., 2005; Hu and Marcucio, 2009; Hu et al., 2015; Xavier et al., 2016). Demonstrating clinical relevance, we have shown that transient *in utero* exposure to the Shh pathway inhibitor cyclopamine causes lateral clefts of the lip that typically extend into the primary and secondary palate, and that this model recapitulates human non-syndromic cleft lip with or without cleft palate (CL/P) (Lipinski et al., 2008b, 2010, 2014). Here, we utilized this pathway-specific mouse model of cleft lip to identify and investigate the mechanism of action of Shh target genes that mediate normal and abnormal upper lip morphogenesis. Along with providing new insight into the molecular and cellular mechanisms that regulate upper lip development, these studies identify novel candidate human CL/P genes that might contribute to this common human birth defect.

RESULTS

Transient Shh signaling inhibition attenuates outgrowth of the medial nasal process

We first investigated the morphogenesis of cleft lip resulting from transient Shh signaling inhibition by examining mouse embryos exposed *in utero* to cyclopamine or vehicle alone (Fig. 1). Although morphologically indistinguishable from vehicle-exposed embryos at gestational day (GD) 9.25, the medial nasal processes (MNPs) of cyclopamine-exposed embryos appeared deficient by GD10.25 (Fig. 1A,B,E,F). By GD11.0, the lower aspect of the MNP was markedly deficient, preventing contact and subsequent fusion with the maxillary process (Fig. 1C,G). By GD14.0, the majority of cyclopamine-exposed embryos exhibited unilateral or bilateral cleft

[1]Department of Comparative Biosciences, School of Veterinary Medicine, University of Wisconsin-Madison, Madison, WI 53706, USA. [2]Molecular and Environmental Toxicology Center, University of Wisconsin-Madison, Madison, WI 53706, USA. [3]Northwestern University Feinberg School of Medicine and the Developmental Biology and Cancer Biology Programs of the Stanley Manne Children's Research Institute, Chicago, IL 60611, USA. [4]School of Dental Medicine, Department of Oral Biology, Center for Craniofacial and Dental Genetics, University of Pittsburgh, Pittsburgh, PA 15261, USA.

*Author for correspondence (robert.lipinski@wisc.edu)

J.W.Y., 0000-0003-3875-3641; E.J.L., 0000-0002-5735-1712; L.J.A.-W., 0000-0002-8955-117X; M.L.M., 0000-0002-2648-2832; R.J.L., 0000-0002-1994-4090

Received 28 January 2017; Accepted 24 April 2017

Development (2017) 144, 2082-2091 doi:10.1242/dev.149930

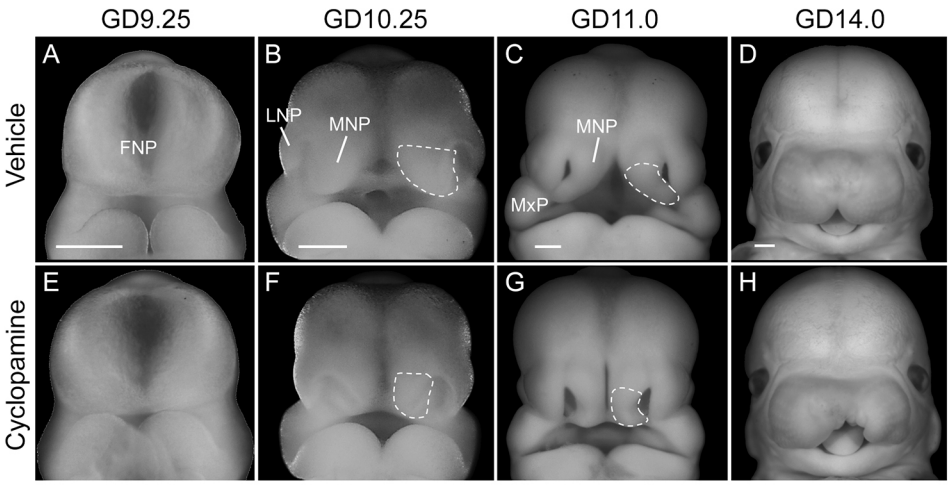

Fig. 1. Transient Shh signaling inhibition causes cleft lip due to a deficiency of the medial nasal process. Representative mouse embryos exposed to vehicle (A-D) or cyclopamine (E-H) are shown at the indicated stages of development (*n*=3 embryos from two independent litters per stage per treatment). The medial nasal process (MNP) is outlined. Note the deficient frontonasal prominence (FNP)-derived MNP of a cyclopamine-exposed embryo at GD10.25 that precludes fusion with the maxillary process (MxP) at GD11.0, leading to unilateral (shown in H) or bilateral cleft lip visible at GD14.0. LNP, lateral nasal process. Scale bars: 300 µm.

lip in the absence of other gross craniofacial malformations (Fig. 1D,H).

Identification of Shh-regulated genes in upper lip morphogenesis

To define the temporal dynamics of transient Shh signaling inhibition during CL/P pathogenesis, we assessed expression of the conserved Shh target gene *Gli1* by *in situ* hybridization (ISH). Whereas no apparent difference was observed at GD9.0, *Gli1* expression was markedly reduced in the ventral frontonasal prominence (FNP) of cyclopamine-exposed embryos by GD9.25 (Fig. 2A,B). Both the medial and lateral nasal processes develop from swellings of the FNP. To identify targets of Shh signaling during the initial pathogenesis of CL/P, FNP tissue was microdissected from stage-matched vehicle- and cyclopamine-exposed GD9.25 embryos (Fig. 2B, outlined) and subjected to cDNA microarray analysis. Of 210 significantly dysregulated genes that were identified, 120 were increased and 90 were decreased by cyclopamine exposure. Networking and gene annotation enrichment analyses confirmed Shh pathway modulation and revealed significant enrichment of the Forkhead box (Fox) family of transcription factors, with multiple members appearing dysregulated during the initial pathogenesis of cleft lip (Fig. 2C).

RT-PCR analysis confirmed significant downregulation of the Shh target genes *Gli1* and *Ptch1*, as well as nine Fox family members: *Foxa2*, *Foxb2*, *Foxc1*, *Foxc2*, *Foxd1*, *Foxe1*, *Foxf1*, *Foxf2* and *Foxl1* (Fig. 2D). Two additional Fox members (*Foxm1* and *Foxo1*) expressed in the FNP were not differentially expressed in the microarray or as assessed by RT-PCR. These findings demonstrate that inhibition of Shh signaling results in downregulation of a specific subset of Fox genes during cleft lip pathogenesis.

Shh pathway activity and *Foxf2* expression correspond with mesenchymal cell proliferation in the MNP

We next characterized the spatiotemporal expression domains of the identified Fox genes during early upper lip development. Because SHH ligand from the ectoderm signals to adjacent cranial neural crest cell (cNCC)-derived mesenchyme, we focused on Fox genes expressed in the mesenchyme of the FNP and MNP. Section ISH analysis revealed seven Fox genes expressed in the mesenchyme of the ventral FNP: *Foxb2*, *Foxc1*, *Foxc2*, *Foxd1*, *Foxf1*, *Foxf2* and *Foxl1* (Fig. 3). In most cases, expression persisted through GD10 and GD11 in the mesenchyme of the MNP tissue that forms the median aspect of the upper lip. The expression domains of *Foxf1* and *Foxf2* closely approximated with that of the canonical Shh target gene *Gli1*. As previously reported, *Foxa2* expression was localized to the neuroectoderm, while *Foxe1* expression was observed in the surface ectoderm of the facial primordia (data not shown) (Moreno et al., 2009; Ruiz i Altaba et al., 1993; Sasaki and Hogan, 1994).

Single-nucleotide polymorphisms (SNPs) in *FOXF2* were recently associated with non-syndromic CL/P in an Asian population (Bu et al., 2015). While *Foxf2* has an intrinsic role in secondary palate development, its role in upper lip development and cleft lip pathogenesis had not been described (Wang et al., 2003; Xu et al., 2016; Nik et al., 2016). We therefore further examined the expression of *Foxf2* during upper lip morphogenesis in our mouse model. *Foxf2* colocalized with both *Gli1* and *Ptch1* in the mesenchyme of the MNP, where they are expressed in a medial-lateral gradient (Fig. 4A,C,E). Expression of these genes remained downregulated at GD10.25 following cyclopamine exposure (Fig. 4B,D,F).

We next investigated the cellular basis of the MNP deficiency upon cyclopamine exposure by staining GD10.25 embryos for the proliferative marker Ki67. Following cyclopamine exposure, a reduction of proliferating cells was observed in the mesenchymal domain of the medial portion of the MNP that normally has the highest expression of *Gli1*, *Ptch1* and *Foxf2* (Fig. 4G,H). Quantification of Ki67-positive cells confirmed a tissue-specific reduction in cellular proliferation affecting the mesenchyme of the MNP but not the adjacent surface ectoderm or the neuroectoderm (Fig. S1). Multipotent cNCCs give rise to the mesenchyme of the MNPs as well as the neighboring lateral nasal processes that form the lateral aspects of the nostrils. However, reduced proliferation of cNCC-derived mesenchyme appeared specific to the MNP, consistent with the observation that cyclopamine exposure attenuates outgrowth of the MNPs without affecting morphogenesis of the lateral nasal processes (Fig. 1).

Foxf2 is a target of canonical Shh signaling in cNCCs

We then examined how Shh signaling regulates *Foxf2* in the tissues that form the upper lip. Consistent with paracrine signaling activity and expression data shown in Fig. 4, we found that *Shh*, which encodes a secreted ligand, is expressed in the surface ectoderm of the MNP, whereas *Gli1* and *Foxf2* are predominantly expressed in the adjacent mesenchyme (Fig. 5A). To decipher how Shh signaling regulates *Foxf2* at the cellular level, we utilized a mouse cNCC line

Development (2017) 144, 2082-2091 doi:10.1242/dev.149930

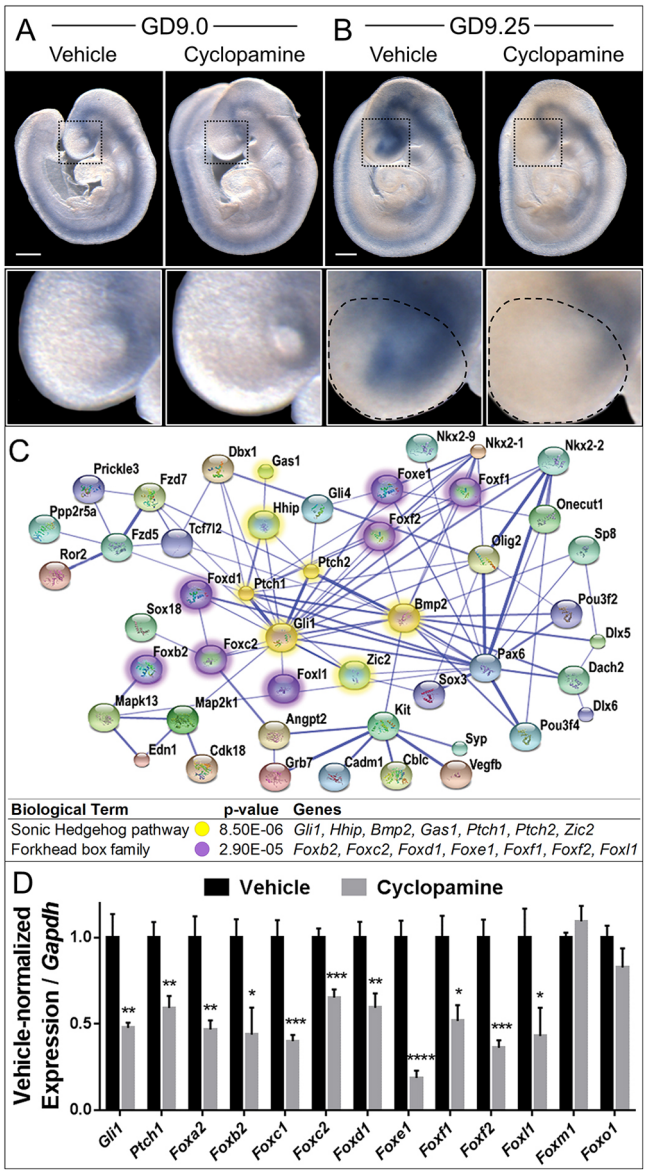

Fig. 2. Shh regulates Fox genes in cleft lip pathogenesis. (A,B) Stage-matched GD9.0 (A) and GD9.25 (B) embryos exposed *in utero* to vehicle or cyclopamine and subjected to ISH for *Gli1*. The boxed region of the FNP is magnified beneath. Although *Gli1* expression is grossly similar at GD9.0, downregulation of *Gli1* is apparent in cyclopamine-exposed embryos by GD9.25. The microdissected FNP region used for the microarray and subsequent RT-PCR validation is outlined on the GD9.25 embryos. Scale bars: 300 µm. (C) A STRING network of select significantly differentially expressed genes identified by microarray. Colored nodes represent significant dysregulated genes; blue edges show functional and predicted interactions between gene products, with the thicker, darker lines representing interactions for which evidence is more abundant. Note the high degree of centrality of Shh signaling pathway genes (yellow) and Forkhead box (Fox) transcription factor genes (purple). *P*-value indicates significant enrichment for the Shh pathway and Fox family within the dysregulated gene set. (D) RT-PCR validation of the indicated genes in vehicle-exposed or cyclopamine-exposed FNP tissue. Values represent mean±s.e.m. expression of the cyclopamine-exposed group relative to *Gapdh*, normalized to the vehicle control group (n=6 pooled litters per group). **P*<0.05, ***P*<0.01, ****P*<0.001, *****P*<0.0001 (two-tailed *t*-test with Holm-Sidak correction).

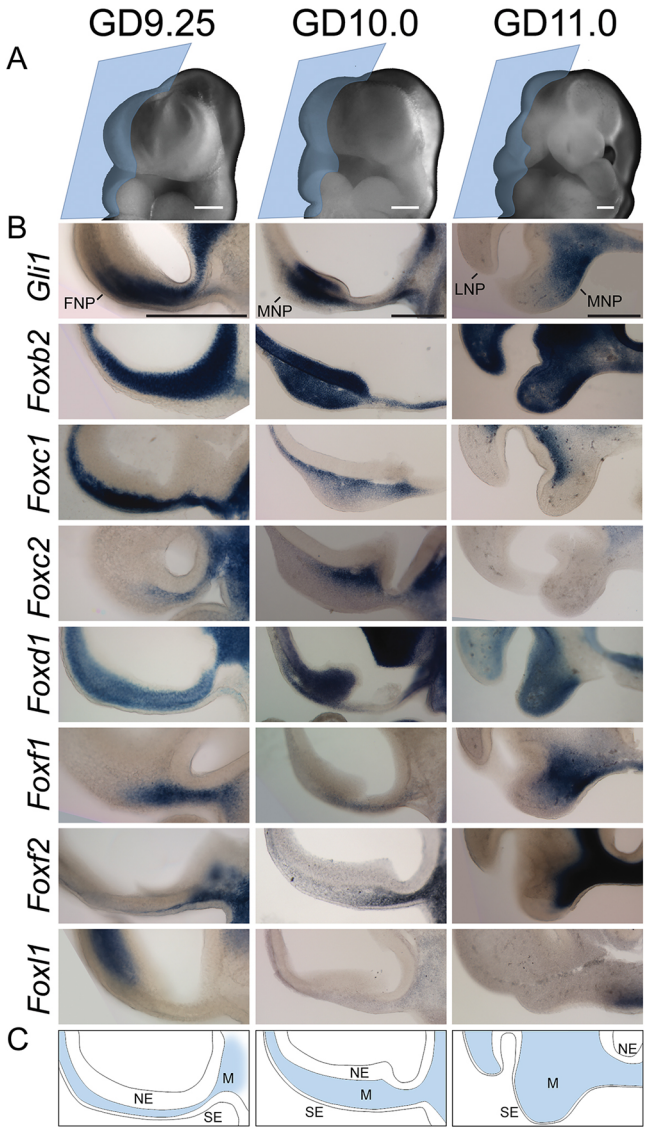

Fig. 3. Fox gene expression during upper lip development. (A) Oblique images of untreated GD9.25, GD10 and GD11 embryos illustrate the plane of section (blue trapezoids) in the panels beneath. (B) Representative images are shown for n=3 embryos from at least two independent litters per gene per stage. *Gli1* and seven Fox genes are expressed in the mesenchyme of the tissues that form the upper lip, i.e. the FNP at GD9.25 and MNP at GD10 and GD11. (C) Schematic showing tissue compartments of the developing face and brain at GD9.25, GD10 and GD11. FNP, frontonasal prominence; MNP, medial nasal process; SE, surface ectoderm; M, mesenchyme; NE, neuroectoderm. Scale bars: 200 µm.

(O9-1) that recapitulates the expression signature [*AP-2α* (*Tfap2a*), *Twist1*, *Sox9*, *Cd44*] and differentiation potential of the post-migrational neural crest-derived cranial mesenchyme (Ishii et al., 2012). Shh ligand (SHH) stimulation of cNCCs caused significant upregulation of both *Gli1* and *Foxf2* expression, which was blocked completely by the addition of vismodegib (Fig. 5B). Both vismodegib and cyclopamine act by binding to and inhibiting the Shh pathway transducing protein smoothened (SMO) (Robarge et al., 2009; Heyne et al., 2015). Because blocking SMO activity prevented induction of *Foxf2*, we next tested whether SMO overexpression could activate *Foxf2* expression. Overexpression of a mutant form of human *SMO* (*SMO*^{M2}) that generates constitutive downstream pathway activity (Xie et al., 1998) was sufficient to induce both *Gli1* and *Foxf2* expression to levels approximating SHH ligand stimulation (Fig. 5C). SMO acts

Development (2017) 144, 2082-2091 doi:10.1242/dev.149930

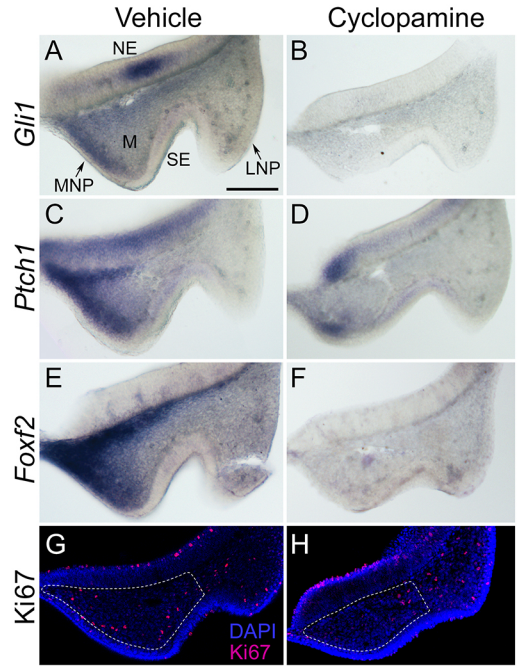

Fig. 4. Concomitant downregulation of *Gli1*, *Ptch1* and *Foxf2* parallels reduced cell proliferation in the MNP during cleft lip pathogenesis. (A-F) Frontal sections through the MNP and LNP of GD10.25 embryos exposed *in utero* to vehicle or cyclopamine and subjected to ISH for *Gli1* (A,B), *Ptch1* (C,D) or *Foxf2* (E,F). *Gli1* and *Ptch1* colocalize with *Foxf2* in the MNP, and each is downregulated during cleft lip pathogenesis. (G,H) Immunostaining for Ki67 (magenta) and DAPI staining (blue) in the same plane of section shows that reduced proliferation is most apparent in the domain of *Gli1*, *Ptch1* and *Foxf2* expression following cyclopamine exposure. Dashed lines delineate mesenchyme of the MNP. MNP, medial nasal process; LNP, lateral nasal process; NE, neuroectoderm; M, mesenchyme; SE, surface ectoderm. Scale bar: 300 µm.

upstream of three GLI proteins that regulate the transcription of canonical Shh target genes. To test whether GLI activity is required for transcriptional regulation of *Foxf2*, we expressed a dominant-negative form of GLI2, the primary transcriptional activator of Shh target genes (Roessler et al., 2005; Lipinski et al., 2006). In cNCCs expressing dominant-negative *GLI2* (dn*GLI2*), *Gli1* and *Foxf2* expression was not significantly changed by the addition of SHH ligand (Fig. 5D).

The zinc-finger proteins GLI1, GLI2 and GLI3 regulate the transcription of canonical Shh target genes by binding to GLI consensus binding sites in the DNA (Kinzler and Vogelstein, 1990; Yoon et al., 2002). Putative GLI-binding sites conserved between mouse and human were identified within a 20 kb region surrounding *Foxf2*. A conserved GLI-binding site containing two mismatches was identified 0.8 kb downstream from the *Foxf2* coding sequence (Fig. 6B). We used electrophoretic mobility shift assays (EMSAs) to test whether this putative GLI-binding site can directly interact with GLI1 protein. Digoxigenin (DIG)-labeled oligonucleotide probes were synthesized for the identified sequence downstream of *Foxf2* and control sequences. Purified GLI1 physically bound the sequence downstream of *Foxf2*, as well as a known GLI-binding site upstream of *Foxl1* (Madison et al., 2009), causing each band to shift (Fig. 6A). The specificity of GLI1 binding to *Foxf2* and *Foxl1* was confirmed by competing away GLI1 from each DIG-labeled oligonucleotide probe using unlabeled probe. This competition was not observed with non-specific competitor probes with mutated GLI-binding sites. An additional putative GLI-binding site downstream of *Foxb2* did not shift in the presence of GLI1, further supporting the specificity of the sequence identified downstream of *Foxf2*.

Shh-Foxf2 signaling promotes cNCC proliferation

Our *in vivo* data demonstrate that cleft lip resulting from transient Shh pathway inhibition follows concomitant decreases in cell proliferation and *Foxf2* expression in the cNCC-derived MNP mesenchyme. We therefore tested whether Shh-Foxf2 signaling directly regulates cNCC proliferation. SHH ligand stimulation of wild-type cNCCs resulted in a 36% increase in cell number compared with the control. Consistent with the transcriptional response of *Foxf2* to SHH ligand stimulation, the increase in cell proliferation was blocked by addition of the SMO antagonist vismodegib (Fig. 7A). To test the specific role of *Foxf2* in regulating the proliferative response of cNCCs, we expressed either full-length *FOXF2* or a truncated form that acts as a dominant negative (Ormestad et al., 2006) in wild-type cNCCs. Transient overexpression of full-length *FOXF2* (*pEVRF0-FOXF2*) caused a 33% increase in cell number relative to cells transfected with empty *pEVRF0* vector (Fig. 7B). Conversely, stable overexpression of dominant-negative *FOXF2* dampened the proliferative response of cNCCs stimulated with SHH ligand as compared with control cells overexpressing empty *pLenti* vector only (Fig. 7C).

FOXF2 SNPs are associated with human cleft lip

Mutations in *FOXF2* have recently been linked to CL/P in humans, but existing studies are for a single Asian population (Bu et al., 2015). To assess the broader relevance of this gene in human clefting, we examined the *FOXF2* locus within a large, multi-ethnic population of individuals with non-syndromic OFCs. We selected common SNPs within *FOXF2* and a 30 kb flanking region. A cluster of SNPs located downstream of *FOXF2* were associated with CL/P (lead SNP rs71697177, $P=1.47\times10^{-5}$) (Fig. S2). We then stratified the CL/P sample into those with a cleft of the upper lip only (CL) and those with cleft lip and cleft palate (CLP) (Table 1). The downstream peak associated with CL/P appeared more strongly associated with CLP (rs71697177, $P_{CLP}=1.85\times10^{-4}$ and $P_{CL}=0.021$). In the CL analysis, the most significant *P*-values were found for several SNPs upstream of *FOXF2* (lead SNP rs1737766, $P=1.13\times10^{-3}$), although these were not formally significant after corrections for multiple testing. To account for discordant sample sizes between the CL and CLP analyses, we performed a formal test of the differences in effects of the top SNPs in each analysis. Whereas the rs1737766 association was specific to CL ($OR_{CL}=1.39$, $OR_{CLP}=0.93$; $P=0.0003$), there was no difference in effect for rs71697177 ($OR_{CL}=0.64$, $OR_{CLP}=0.72$; $P=0.29$).

DISCUSSION

Shh signaling is a master regulator of the epithelial-mesenchymal interactions that drive orofacial development, but specific targets of the pathway in upper lip development had not been identified. In this study, we leveraged a mouse model of transient *in utero* inhibition of the Shh signaling pathway to investigate genetic and cellular drivers of lip morphogenesis and cleft lip pathogenesis. Whole-transcriptome expression profiling identified significant downregulation of canonical Shh pathway members, as well as multiple Fox family members during the initial pathogenesis of cleft lip. The defining feature of Fox transcription factors is a Forkhead, or winged-helix, DNA-binding domain. This family includes 44 genes in the mouse genome, with each having a close human ortholog (Jackson et al., 2010). Fox genes have been identified as targets of Shh signaling in diverse developmental contexts,

Development (2017) 144, 2082-2091 doi:10.1242/dev.149930

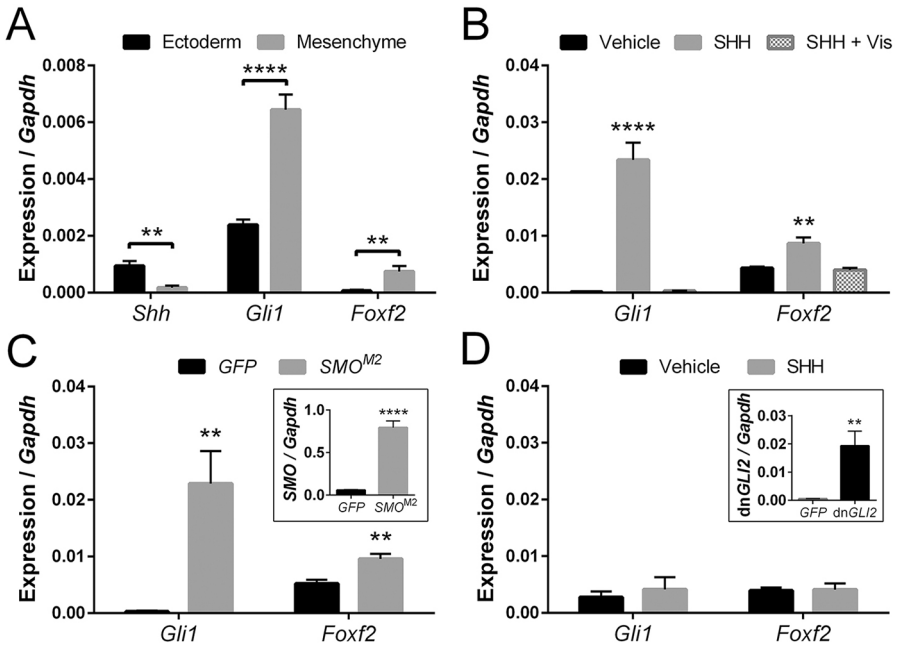

Fig. 5. *Foxf2* is a target of Shh signaling in cranial neural crest cells (cNCCs). (A) Tissue-specific gene expression was determined for isolated GD11 MNP mesenchyme and surface ectoderm. *Shh* was more highly expressed in the MNP surface ectoderm, whereas *Gli1* and *Foxf2* were more highly expressed in the MNP mesenchyme (n=6 pooled litters per group). (B) Gene expression was determined for cNCCs cultured with or without SHH ligand and with or without the SMO antagonist vismodegib (Vis). SHH ligand caused an increase in *Gli1* and *Foxf2* expression, which was blocked by the addition of vismodegib (n=5). (C) Expression of *Gli1* and *Foxf2* are increased in cNCCs overexpressing a constitutively active form of human smoothened (*SMO*^{M2}) relative to *GFP* only (control) (n=5). Inset shows *SMO* expression relative to *Gapdh* in *GFP* (control) and *SMO*^{M2}-*GFP*-overexpressing cells. (D) Expression of *Gli1* and *Foxf2* is unchanged by SHH ligand treatment in cNCCs overexpressing a dominant-negative form of GLI2 (dn*GLI2*) (n=5). Inset shows mean±s.e.m. expression of dn*GLI2* relative to *Gapdh* in vehicle-treated *GFP*-expressing (control) and dn*GLI2*-expressing cells. For all analyses, mean±s.e.m. expression relative to *Gapdh* is shown. **P<0.01, ****P<0.001 (two-tailed t-test with Holm-Sidak correction).

including the gut and central nervous system, while GLI consensus binding sites have been identified in *Foxa2*, *Foxe1*, *Foxf1* and *Foxl1* (Madison et al., 2009; Eichberger et al., 2004; Sasaki et al., 1997).

Our study provides the first evidence that Shh signaling regulates multiple Fox genes during upper lip development and cleft lip pathogenesis. Transcriptional regulation of Fox genes by Shh signaling in facial morphogenesis was first reported by Jeong et al. (2004), who generated mice with conditional pathway inactivation in *Wnt1*-expressing cNCCs. However, in this previous study only five Fox family members were investigated, and affected embryos exhibited near-complete facial truncation, precluding examination of upper lip development. Here, we show that nine individual Fox genes are expressed in the ventral FNP and are downregulated during the initial pathogenesis of cleft lip resulting from temporally

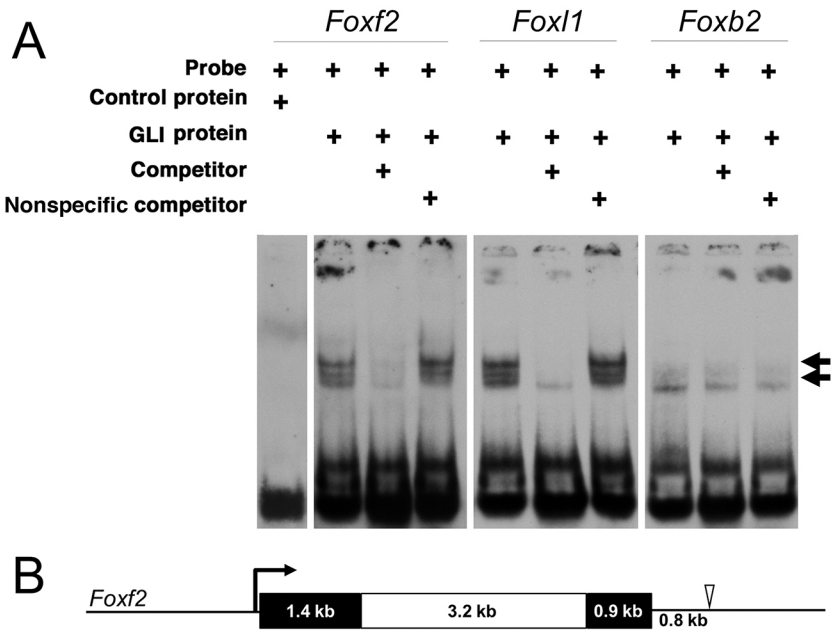

Fig. 6. A novel GLI-binding site at the *Foxf2* locus. (A) EMSAs were used to assess putative GLI-binding sites identified *in silico*. EMSAs of control and three unique putative GLI-binding sites near *Foxf2*, *Foxl1* and *Foxb2*. Arrows indicate shifted bands marking DIG-labeled oligonucleotide probes bound by recombinant GLI1 protein. Lowest band (no arrow) marks free, unbound probe. An oligonucleotide probe containing a putative GLI-binding site 0.8 kb downstream of *Foxf2* was bound by GLI1, causing a band shift. As a positive control, a probe was designed containing a known GLI-binding site near *Foxl1*, which was also bound by GLI1, causing a band shift. A probe containing a putative GLI-binding site near *Foxb2* was not bound by GLI1. Consolidated gel images are shown. (B) A scale-drawn schematic of the mouse *Foxf2* locus. Black boxes denote exons and a white box denotes the intron. The open arrowhead indicates the location of the novel GLI1 binding site 0.8 kb downstream of the *Foxf2* coding sequence.

Development (2017) 144, 2082-2091 doi:10.1242/dev.149930

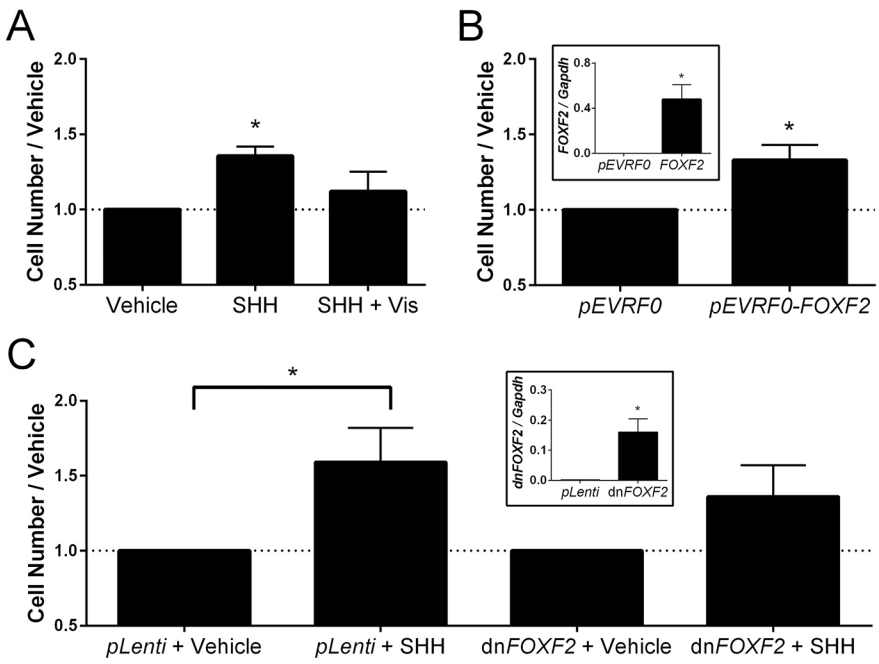

Fig. 7. *Foxf2* promotes cNCC proliferation. (A) cNCCs were cultured with or without SHH ligand and with or without vismodegib (Vis). SHH ligand caused cNCCs to proliferate, which was blocked by addition of vismodegib (n=4). (B) Transient overexpression of full-length *FOXF2* resulted in a significant increase in cell number relative to control (transfected with empty *pEVRF0*) (n=4). Inset shows *FOXF2* expression relative to *Gapdh* in *pEVRF0* (control) and *FOXF2*-overexpressing cells (n=4). (C) In cNCCs with stable overexpression of an empty *pLenti* vector, SHH ligand stimulation caused a significant increase in cell number. In cNCCs with stable overexpression of a dominant-negative form of *FOXF2* (dn*FOXF2*), the change in cell number following SHH ligand stimulation was not statistically significant (P=0.09, n=4). Inset shows dn*FOXF2* expression relative to *Gapdh* in *pLenti* (control) and dn*FOXF2*-overexpressing cells (n=4). Mean±s.e.m. cell count is shown. *P<0.05 (two-tailed t-test).

specific inhibition of the Shh pathway. Seven of these Fox genes exhibit dynamic expression domains in the cNCC-derived mesenchyme of the MNPs that form the median aspect of the upper lip. The expression domain of *Foxf2* in particular parallels that of the canonical Shh target gene *Gli1*.

We show in mouse cNCCs (Ishii et al., 2012) that Shh pathway activation via addition of SHH ligand or overexpression of a constitutively active form of the pathway transducer SMO causes increased *Foxf2* expression, and that this induction requires GLI2. *In silico* screening identified a novel GLI consensus binding site 0.8 kb downstream of *Foxf2*, and we show that purified GLI1 protein directly binds to this site *in vitro*. The EMSA utilized here has proven successful in identifying functional GLI-binding sites that regulate now well-recognized GLI targets such as *Ccnd2* and *Igfbp6* (Yoon et al., 2002; Lipinski et al., 2005; Xu et al., 2009; Lan and Jiang, 2009). Taken together, these data argue that *Foxf2* is a direct target of canonical SHH-SMO-GLI signaling in post-migrational cNCCs.

Formation of the upper lip requires orchestrated growth and fusion of the bilaterally paired medial nasal and maxillary processes (Jiang et al., 2006). Therefore, clefts of the lip can arise from several distinct cellular and morphological mechanisms affecting the medial nasal and/or maxillary processes. We found that expression of several genes expressed in the surface ectoderm that are required for fusion of the medial nasal and maxillary processes [*Pbx1-3*, several Wnt genes, *Tp63* (*Trp63*), *Irf6*] were not changed during cyclopamine-induced cleft lip (Fig. S3). This suggests that these genes are not regulated by Shh signaling, although it is possible that they act upstream of *Shh* in the surface ectoderm. Our observations support the alternative mechanism that epithelial SHH ligand induces pathway activity in the adjacent cNCC mesenchyme and that pathway inhibition reduces proliferation of the cNCC-derived mesenchymal cells of the MNP, causing a tissue deficiency that prevents contact with the opposing maxillary processes, resulting in cleft lip. Consistent with this *in vivo* observation, we show that direct addition of SHH ligand stimulates mouse cNCC proliferation *in vitro*. Moreover, transient overexpression of *FOXF2* is sufficient to induce cNCC proliferation. Overexpression of a dominant-negative form of *FOXF2* dampens the proliferative response of cNCCs to SHH ligand, such that the change is not statistically significant. Partial responsiveness might be explained by functional compensation by other Fox members, such as *Foxf1*, as has been described in other developmental contexts (Xu et al., 2016; Madison et al., 2009). Taken together, these data suggest that post-migrational cNCC proliferation in the MNP is dependent, at least in part, on SHH-mediated induction of *Foxf2*.

The studies described herein are the first to link *Foxf2* to cleft lip pathogenesis in an animal model. Interestingly, *Foxf2* null mice do not exhibit cleft lip but cleft palate only (CPO) (Wang et al., 2003). Functional compensation by other Fox genes might explain this dichotomy. At the same time, relative to humans, the mouse appears resistant to cleft lip, which may mask important developmental regulators of upper lip morphogenesis, such as *Foxf2*. In fact, the majority of mouse OFC models exhibit CPO, even those involving disruption of genes associated with both CPO and CL/P in humans, such as *FOXE1* and *IRF6* (Gritli-Linde, 2008; Juriloff and Harris, 2008; Leslie et al., 2016b; Ludwig et al., 2014). Although these OFC subtypes are traditionally considered distinct, development of the upper lip and secondary palate each involves outgrowth and

Table 1. Top association results for *FOXF2* in a multi-ethnic population with CL/P

				CL/P			CL			CLP		
SNP	Genomic location	Allele 1	Allele 2	*P*	OR	95% CI	*P*	OR	95% CI	*P*	OR	95% CI
rs1737766	1361844	T	C	0.87	1.1	0.91-1.11	1.13×10^{-3}	1.4	1.14-1.70	0.23	0.9	0.83-1.04
rs71697177	1404157	A	AACAC	1.46×10^{-5}	0.7	0.59-0.82	0.021	0.6	0.43-0.93	1.85×10^{-4}	0.7	0.60-0.85

CL/P, cleft lip with or without cleft palate; CL, cleft lip only; CLP, cleft lip and palate. *P*-value by logistic regression; OR, odds ratio; CI, confidence interval.

Development (2017) 144, 2082-2091 doi:10.1242/dev.149930

fusion of facial growth centers that are largely composed of cNCC-derived mesenchyme (Jiang et al., 2006; Lan et al., 2015).

Comparison of our findings in upper lip development with recent evidence that *Foxf2* plays an intrinsic role in secondary palate development suggests a divergence in the genetic regulation of these structures. Xu et al. (2016) found that SHH ligand from the palatal epithelium drives *Foxf2* expression in the adjacent mesenchyme, which then suppresses mesenchymal *Fgf18* expression. This results in loss of *Shh* expression in the palatal shelf epithelium and in CPO (Xu et al., 2016). Suggesting a likely parallel mechanism, Nik et al. (2016) found that *Foxf2* expression regulates TGFβ signaling activity in the cNCC-derived mesenchyme of the secondary palate. Disruption of TGFβ signaling in these cells has been shown to cause defective proliferation, resulting in cleft palate (Iwata et al., 2012). However, these mechanisms do not appear to be conserved in upper lip morphogenesis. Neither *Fgf18* nor markers of TGFβ signaling (*Tgfbr3* and *Itgb1*) were altered during the initial pathogenesis of cyclopamine-induced cleft lip or following SHH ligand stimulation or downstream pathway activation in cNCCs *in vitro* (Fig. S4). Moreover, the proliferative response of cNCCs to SHH ligand or *FOXF2* overexpression occurs without parallel changes in gene expression of *Tfgbr3* or *Itgb1*. This suggests that although regulation of *Foxf2* by Shh signaling is conserved between upper lip and secondary palate development, the downstream targets of FOXF2 that mediate its biological effects are context dependent. Identifying the unique transcriptional targets of FOXF2 in upper lip development is an important area of future investigation that could reveal additional mechanistic insights into cleft lip pathogenesis.

Increasing evidence from genetic association studies suggests that CL and CLP may have distinct risk factors in humans. This includes a locus near *SPRY2* that is more strongly associated with CLP, a locus near *GREM1* that appears to be associated with cleft lip and cleft soft palate, and the *IRF6* enhancer variant that is more strongly associated with CL than CLP (Ludwig et al., 2012; Jia et al., 2015). Our results suggest that CL/P-associated SNPs downstream of *FOXF2* are associated with both CL and CLP. However, we also identified evidence of association for several SNPs upstream of *FOXF2* that appeared specific to CL. Although a biological mechanism behind stronger associations with specific cleft types remains generally elusive, our data suggest that the downstream targets of FOXF2 that mediate its biological effects are context dependent. The SNPs identified in our large multi-ethnic population have not been previously reported. These new associations, along with those previously reported in an Asian population (Bu et al., 2015), strongly link *FOXF2* to CL/P in humans.

We demonstrate an integrated *in vivo-in vitro-in silico* approach to uncover and define the identity and mechanism of action of genetic regulators of upper lip development with relevance to human birth defects. In addition to *Foxf2*, the utility of this approach is underscored by our identification of *Foxe1* as one of the genes most strongly downregulated by cyclopamine exposure. *FOXE1* was recently identified as a major OFC locus linked to both CL/P and CPO in human populations (Moreno et al., 2009; Ludwig et al., 2014). In addition to *Foxf2* and *Foxe1*, our study identifies seven other Fox genes that are downregulated during the initial pathogenesis of cleft lip. Inactivation of two of these genes (*Foxc2* and *Foxf1*) is known to cause CPO in mouse, but examination of these genes in upper lip development has not been presented. For most of the other Fox genes that we have identified as Shh targets during cleft lip pathogenesis, knockout models have not been developed, or analysis of upper lip morphogenesis is precluded by early embryonic lethality. Further investigation of these genes, along with *Foxf2*, will improve our understanding of the mechanisms that regulate upper lip development and illuminate the complex etiology of CL/P in humans.

MATERIALS AND METHODS

Animals

This study was conducted in strict accordance with recommendations in the Guide for the Care and Use of Laboratory Animals of the National Institutes of Health. The protocol was approved by the University of Wisconsin School of Veterinary Medicine Institutional Animal Care and Use Committee (protocol number 13–081.0). Eight-week-old wild-type C57BL/6J mice (*Mus musculus*, Linnaeus) were purchased from The Jackson Laboratory and housed under specific pathogen-free conditions in disposable, ventilated cages (Innovive, San Diego, CA, USA). Rooms were maintained at 22±2°C and 30-70% humidity on a 12-h light, 12-h dark cycle. Mice were fed 2920x Irradiated Harlan Teklad Global Soy Protein-Free Extruded Rodent Diet until day of plug, when dams received 2919 Irradiated Teklad Global 19% Protein Extruded Rodent Diet.

Timed pregnancies

One or two nulliparious female mice were placed with a single male for 1-2 h and then examined for copulation plugs. The beginning of the mating period was designated as GD0, and pregnancy was confirmed by assessing weight gain between GD7 and GD10, as previously described (Heyne et al., 2015). Pregnant dams were euthanized at the indicated gestational day ±1 h. Somite number was used as an indicator of embryo gestational stage. For microarray and RT-PCR validation, all analyzed embryos had 20-24 somite pairs, a subset of GD9.25 (Theiler, 1989). For ISH, embryos compared between treatment groups were stage matched ±1 somite pair.

Cyclopamine administration

Pregnant dams were administered 120 mg per kg per day cyclopamine (LC Laboratories, CAS #4449-51-8) or vehicle alone from GD8.25 to ∼GD9.375 using ALZET 2001D micro-osmotic pumps (Cupertino, CA, USA). This subcutaneous infusion exposure model yields steady-state serum concentrations within a few hours after pump implantation (GD8.25) that persist until dispensation is complete (∼GD9.375) (Lipinski et al., 2008b, 2010).

RNA extraction and purification

For *in vivo* assays, microdissected FNP tissues from six cyclopamine-exposed and six vehicle-exposed control litters were pooled by litter. RNA was isolated using GE Illustra RNAspin kits (GE Healthcare). This RNA was used for both microarray and RT-PCR validation assays. cDNA was synthesized from 1 µg total RNA using Promega GoScript reverse transcription reaction kits. Separation of mesenchyme and surface ectoderm of GD11 embryos was accomplished as previously described (Li and Williams, 2013). For separated tissues and *in vitro* cell cultures, cDNA was synthesized from 500 ng total RNA.

Microarray sample preparation, hybridization and scanning

Affymetrix Mouse Gene 2.0 ST GeneChip arrays were used for transcriptome analysis. Labeled cDNA was generated from 100-500 ng total RNA with Ambion Whole-Transcript Expression and Affymetrix GeneChip Whole-Transcript Terminal Labeling Reagents, according to manufacturers' specifications. GeneChips were scanned at 570 nm on an Affymetrix GC3000 G7 scanner, and signals were determined using Affymetrix GCOS and Affymetrix Expression Console software.

Microarray computational analysis

Significant differential gene expression was determined using the Affymetrix Transcriptome Analysis Console (TAC). Gene networking analysis was performed using STRING (Franceschini et al., 2013). Gene annotation enrichment analysis for pathways and biological processes was conducted using the Database for Annotation, Visualization and Integrated Discovery (DAVID) (Huang et al., 2009a,b).

Development (2017) 144, 2082-2091 doi:10.1242/dev.149930

Quantitative real-time RT-PCR

Singleplex RT-PCR was conducted as previously described (Heyne et al., 2016). Primer sequences are listed in Table S1. *Gapdh* was used as the housekeeping gene for expression normalization, and analyses were conducted with the $2^{-\Delta\Delta Ct}$ method.

In situ hybridization (ISH)

ISH analysis was performed as previously described (Heyne et al., 2016), using an established high-throughput technique (Abler et al., 2011). Embryos were processed whole or embedded in 4% agarose gel and cut in 50 µm sections using a vibrating microtome. Embryos were imaged using a MicroPublisher 5.0 camera connected to an Olympus SZX-10 stereomicroscope for whole mount or a Nikon Eclipse E600 microscope for sections. ISH riboprobe primers are listed in Table S2.

Immunohistochemistry

GD10.25 embryos were fixed in 4% paraformaldehyde in PBS overnight prior to graded dehydration into methanol and storage at −20°C. Embryos were subsequently rehydrated into PBS and 100 µm frontal sections were obtained using a vibrating microtome. Sections were blocked in 5% normalized goat serum (NGS) and 1% DMSO in PBSTx (PBS with 0.5% Triton X-100) for 1 h, incubated in monoclonal rabbit anti-Ki67 (1:250; Cell Signaling, #9027) (Gerdes et al., 1983), washed, and transferred to monoclonal goat anti-rabbit Alexa Fluor 594 secondary antibody (1:1000; Thermo Scientific, #R37117) in PBSTx containing 5% NGS for 1 h at room temperature. Finally, sections were incubated with DAPI (1:1000; Thermo Scientific) in PBS for 6 min, and imaged using a Leica SP8 confocal microscope. For Ki67 quantification, a blinded-rater processed each image to reduce background and optimize signal accuracy. Ki67-positive cells/area in each *z*-image were determined using the ImageJ (NIH) cell counter tool.

GLI transcription factor-binding site analysis

Evolutionarily conserved GLI-binding sites between mouse (mm10) and human (Hg19) were identified *in silico* using the VISTApoint tool (Loots et al., 2002). 10 kb regions upstream and downstream of each gene coding sequence were analyzed for GLI, GLI1, GLI2 and GLI3 consensus binding sites. Putative GLI-binding sites with fewer than three mismatches from the consensus GLI-binding sequence (TGGGTGGTC) were accepted for further analysis. GLI-binding sites were confirmed by EMSA using a DIG (digoxigenin) Gel Shift Kit (Roche), according to the manufacturer's specifications. Primers used for probe synthesis are listed in Table S3. Purified recombinant GLI1-protein or PinPoint control protein (Promega) was used for these assays. Samples were separated by electrophoresis on a 5% TBE gel (Bio-Rad), transferred onto a Zeta Probe GT membrane (Bio-Rad), and UV cross-linked. Probes were targeted using an anti-DIG, alkaline phosphatase-conjugated antibody (Roche). Specific protein-DNA complexes were visualized using ready-to-use CSPD chemiluminescent substrate (Roche).

In vitro cell culture

Immortalized O9-1 mouse cNCCs were cultured as described (Ishii et al., 2012). Cells were authenticated and tested for contamination. For treatment, O9-1 cells were plated at 5×10^5 cells/ml (0.4 ml per well in a 24-well plate) and allowed to attach in complete 15% FBS media for 24 h before media were replaced with DMEM containing 1% FBS with or without SHH-N ligand (R&D Systems) at 0.4 µg/ml and with or without 100 nM vismodegib (LC Laboratories, CAS No 879085-55-9) dissolved in DMSO.

Stable transfection experiments

O9-1 cells overexpressing *GFP*, *SMO^{M2}-GFP* and dn*GLI2-RFP* (GLI2-mutB) were generated as described (Lipinski et al., 2008a). A *pIRES* shuttle vector carrying coding sequences for *GFP*, *SMO^{M2}-GFP* and *GLI2mutB-RFP* was used to retrovirally infect wild-type O9-1 cells. Cells were plated at subconfluence in DMEM with 10% FBS. Cells were incubated with viral-conditioned medium at 37°C for 6 h. Following a 72 h propagation period, appropriate GFP$^+$ or RFP$^+$ populations were isolated using a BD FACSAria III fluorescence-activated cell sorter. Stably transfected cells were plated at 5×10^5 cells/ml (0.4 ml per well in a 24-well plate). After 24 h, cells were treated with DMEM containing 1% FBS with or without SHH-N ligand for 48 h. Cell lysates were collected for RNA extraction. Stable dn*FOXF2*-overexpressing O9-1 cells were created using *pLenti* CMV Blast empty vector (w263-1; Addgene plasmid #17486), provided by Dr Eric Campeau (Campeau et al., 2009). Dominant-negative *FOXF2* (*pGFP*-C1-dn*FOXF2*) was provided by Dr Peter Carlsson (Hellqvist et al., 1996, 1998). The dn*FOXF2* fragment was removed from the *pGFP*-C1 backbone with *Bam*HI and *Xba*I sites and then inserted using the same sites into the *pLenti* CMV Blast empty transfer plasmid. A negative control cell line was generated in parallel by infecting with the empty *pLenti* CMV Blast vector. Infected cells were selected by blasticidin S. Cells were plated at 2×10^5 cells per well of a 24-well plate in duplicate. After 24 h, cells were treated with DMEM containing 1% FBS with or without SHH-N ligand for 48 h. Cell lysates were collected for RNA extraction or counted with a hemocytometer.

Transient transfection experiments

Full-length *FOXF2* (*pEVRF0-FOXF2*) was provided by Dr Peter Carlsson (Hellqvist et al., 1996, 1998). Negative control (*pEVRF0* empty vector) was made by removing *FOXF2* with *Bam*HI and *Sac*I and religating with a short noncoding sequence. O9-1 cells were plated at 1.25×10^5 cells/ml (0.4 ml per well in a 24-well plate) in duplicate. After 24 h, media were changed to DMEM with 1% FBS and transiently transfected with 0.75 µl Lipofectamine 3000 (Thermo Fisher Scientific), 1 µl P3000 reagent (Thermo Fisher Scientific) and 500 ng *pEVRF0-FOXF2* or *pEVRF0* empty vector in Opti-MEM (Gibco) following manufacturer's instructions. After 48 h, cell lysates were collected for RNA extraction or counted by hemocytometer.

Statistics

Affymetrix TAC was used for determination of significant differential expression in microarray experiments, utilizing an FDR *P*-value of 0.5 (Benjamini-Hochberg) based on independent RT-PCR validation. DAVID was used for determination of significant enrichment of differentially expressed genes (Huang et al., 2009a,b). Two-tailed *t*-tests with Holm-Sidak correction were used to determine whether gene expression was changed by cyclopamine exposure *in vivo* or with SHH ligand stimulation with or without vismodegib in O9-1 cNCCs. Two-tailed *t*-tests were used for analysis of proliferation assays and tissue-specific gene expression. GraphPad Prism 6 was used for all non-microarray statistical analyses. An alpha value of 0.05 was maintained for determination of significance for all non-microarray experiments.

Human genetics analysis

The cohort for this association analysis comes from a world-wide, multi-ethnic recruitment in the Pittsburgh Orofacial Cleft (POFC) study. University of Pittsburg Institutional Review Board approval and informed consent was obtained for all subjects. Participants comprising 823 CL/P cases, 1700 controls and 1319 case-parent trios were recruited from 13 countries worldwide. Full details of the recruitment, genotyping and quality control procedures have been described previously (Leslie et al., 2016a). Briefly, samples were genotyped on the Illumina HumanCore+Exome array, phased with SHAPEIT2, and imputed to 1000 Genomes Phase 3 reference panel. Genotype probabilities were converted to most-likely genotypes using Plink v1.9 if the genotype with the highest probability was >0.9. SNPs with minor allele frequencies <1%, INFO score <0.5, or deviating from Hardy–Weinberg equilibrium in European controls (P<0.0001) were removed from the analysis. Analysis was further limited to 550 SNPs located within a 66 kb interval (*FOXF2* and 30 kb flanking sequence). Separate analyses for cases and controls (logistic regression assuming an additive genetic model and including 18 principal components of ancestry) and trios (transmission disequilibrium test) were combined in an inverse variance-weighted fixed-effects meta analysis. Analysis was performed for CL/P and stratified into CL and CLP. A Bonferroni *P*-value threshold of 4.3×10^{-4} was considered statistically significant based on 116 independent tests (Gao et al., 2010). Differences in effects between CL and CLP were formally tested using a Q statistic (Schenker and Gentleman, 2001).

Acknowledgements

We thank Drs Mamoru Ishii and Robert Maxson for providing O9-1 cells; Drs Peter Carlsson and Eric Campeau for *FOXF2* and lentiviral plasmid constructs; Galen

Heyne for experimental support; Dr John Svaren for help on binding site analysis; Jenna Carlson, Drs John Shaffer and Eleanor Feingold for association analyses; the UW-Madison Biotechnology Center; the UW-Madison Carbone Cancer Center Flow Cytometry Laboratory; the UW-Madison Biotron Laboratory; and the UW-Madison Research Animals Resource Center.

Competing interests
The authors declare no competing or financial interests.

Author contributions
Conceptualization: J.L.E., R.J.L.; Methodology: J.L.E., D.M.F., J.W.Y., E.J.L., H.M.C.; Formal analysis: J.L.E., D.M.F., J.W.Y., E.J.L., H.W.K.; Investigation: J.L.E., D.M.F., J.W.Y., E.J.L., H.W.K., L.J.A.-W., M.L.M.; Writing - original draft: J.L.E., R.J.L.; Writing - review & editing: J.L.E., D.M.F., H.M.C., R.J.L., L.J.A-W., H.W.K., J.W.Y., D.O.W., E.J.L., M.L.M.; Funding acquisition: M.L.M., R.J.L.

Funding
This work was supported by the National Institutes of Health [R00DE022010-02 to R.J.L., T32ES007015-37 to J.L.E., T35OD011078 to L.J.A.-W., K99DE025060 to E.J.L., X01HG007485 and R01DE016148 to M.L.M.]. Deposited in PMC for release after 12 months.

Data availability
Microarray data generated in this study are available at Gene Expression Omnibus under accession number GSE98336 (https://www.ncbi.nlm.nih.gov/geo/query/acc.cgi?acc=gse98336).

Supplementary information
Supplementary information available online at
http://dev.biologists.org/lookup/doi/10.1242/dev.149930.supplemental

References
Abler, L. L., Mehta, V., Keil, K. P., Joshi, P. S., Flucus, C.-L., Hardin, H. A., Schmitz, C. T. and Vezina, C. M. (2011). A high throughput in situ hybridization method to characterize mRNA expression patterns in the fetal mouse lower urogenital tract. *J. Vis. Exp.* **54**, e2912.

Bu, L., Chen, Q., Wang, H., Zhang, T., Hetmanski, J. B., Schwender, H., Parker, M., Chou, Y.-H. W., Yeow, V., Chong, S. S. et al. (2015). Novel evidence of association with nonsyndromic cleft lip with or without cleft palate was shown for single nucleotide polymorphisms in FOXF2 gene in an Asian population. *Birth Defects Res. A Clin. Mol. Teratol* **103**, 857-862.

Campeau, E., Ruhl, V. E., Rodier, F., Smith, C. L., Rahmberg, B. L., Fuss, J. O., Campisi, J., Yaswen, P., Cooper, P. K. and Kaufman, P. D. (2009). A versatile viral system for expression and depletion of proteins in mammalian cells. *PLoS ONE* **4**, e6529.

Eichberger, T., Regl, G., Ikram, M. S., Neill, G. W., Philpott, M. P., Aberger, F. and Frischauf, A.-M. (2004). FOXE1, a new transcriptional target of GLI2 is expressed in human epidermis and basal cell carcinoma. *J. Invest. Dermatol.* **122**, 1180-1187.

Franceschini, A., Szklarczyk, D., Frankild, S., Kuhn, M., Simonovic, M., Roth, A., Lin, J., Minguez, P., Bork, P., von Mering, C. et al. (2013). STRING v9.1: protein-protein interaction networks, with increased coverage and integration. *Nucleic Acids Res.* **41**, D808-D815.

Gao, X., Becker, L. C., Becker, D. M., Starmer, J. D. and Province, M. A. (2010). Avoiding the high Bonferroni penalty in genome-wide association studies. *Genet. Epidemiol.* **34**, 100-105.

Gerdes, J., Schwab, U., Lemke, H. and Stein, H. (1983). Production of a mouse monoclonal antibody reactive with a human nuclear antigen associated with cell proliferation. *Int. J. Cancer* **31**, 13-20.

Gritli-Linde, A. (2008). The etiopathogenesis of cleft lip and cleft palate: usefulness and caveats of mouse models. *Curr. Top. Dev. Biol.* **84**, 37-138.

Gritli-Linde, A. (2012). The mouse as a developmental model for cleft lip and palate research. *Front. Oral Biol.* **16**, 32-51.

Hellqvist, M., Mahlapuu, M., Samuelsson, L., Enerbäck, S. and Carlsson, P. (1996). Differential activation of lung-specific genes by two forkhead proteins, FREAC-1 and FREAC-2. *J. Biol. Chem.* **271**, 4482-4490.

Hellqvist, M., Mahlapuu, M., Blixt, A., Enerbäck, S. and Carlsson, P. (1998). The human forkhead protein FREAC-2 contains two functionally redundant activation domains and interacts with TBP and TFIIB. *J. Biol. Chem.* **273**, 23335-23343.

Heyne, G. W., Plisch, E. H., Melberg, C. G., Sandgren, E. P., Peter, J. A. and Lipinski, R. J. (2015). A simple and reliable method for early pregnancy detection in inbred mice. *J. Am. Assoc. Lab. Anim. Sci.* **54**, 368-371.

Heyne, G. W., Everson, J. L., Ansen-Wilson, L. J., Melberg, C. G., Fink, D. M., Parins, K. F., Doroodchi, P., Ulschmid, C. M. and Lipinski, R. J. (2016). Gli2 gene-environment interactions contribute to the etiological complexity of holoprosencephaly: evidence from a mouse model. *Dis. Model. Mech.* **9**, 1307-1315.

Hu, D. and Marcucio, R. S. (2009). A SHH-responsive signaling center in the forebrain regulates craniofacial morphogenesis via the facial ectoderm. *Development* **136**, 107-116.

Hu, D., Young, N. M., Li, X., Xu, Y., Hallgrímsson, B. and Marcucio, R. S. (2015). A dynamic Shh expression pattern, regulated by SHH and BMP signaling, coordinates fusion of primordia in the amniote face. *Development* **142**, 567-574.

Huang, D. W., Sherman, B. T. and Lempicki, R. A. (2009a). Bioinformatics enrichment tools: paths toward the comprehensive functional analysis of large gene lists. *Nucleic Acids Res.* **37**, 1-13.

Huang, D. W., Sherman, B. T. and Lempicki, R. A. (2009b). Systematic and integrative analysis of large gene lists using DAVID bioinformatics resources. *Nat. Protoc.* **4**, 44-57.

Ishii, M., Arias, A. C., Liu, L., Chen, Y.-B., Bronner, M. E. and Maxson, R. E. (2012). A stable cranial neural crest cell line from mouse. *Stem Cells Dev.* **21**, 3069-3080.

Iwata, J., Hacia, J. G., Suzuki, A., Sanchez-Lara, P. A., Urata, M. and Chai, Y. (2012). Modulation of noncanonical TGF-β signaling prevents cleft palate in Tgfbr2 mutant mice. *J. Clin. Invest.* **122**, 873-885.

Jackson, B. C., Carpenter, C., Nebert, D. W. and Vasiliou, V. (2010). Update of human and mouse forkhead box (FOX) gene families. *Hum. Genomics* **4**, 345-352.

Jeong, J., Mao, J., Tenzen, T., Kottmann, A. H. and Mcmahon, A. P. (2004). Hedgehog signaling in the neural crest cells regulates the patterning and growth of facial primordia. *Genes Dev.* **18**, 937-951.

Jia, Z., Leslie, E. J., Cooper, M. E., Butali, A., Standley, J., Rigdon, J., Suzuki, S., Gongorjav, A., Shonkhuuz, T. E., Natsume, N. et al. (2015). Replication of 13q31.1 association in nonsyndromic cleft lip with cleft palate in Europeans. *Am. J. Med. Genet. A* **167**, 1054-1060.

Jiang, R., Bush, J. O. and Lidral, A. C. (2006). Development of the upper lip: morphogenetic and molecular mechanisms. *Dev. Dyn.* **235**, 1152-1166.

Juriloff, D. M. and Harris, M. J. (2008). Mouse genetic models of cleft lip with or without cleft palate. *Birth Defects Res. A Clin. Mol. Teratol.* **82**, 63-77.

Kinzler, K. W. and Vogelstein, B. (1990). The GLI gene encodes a nuclear protein which binds specific sequences in the human genome. *Mol. Cell. Biol.* **10**, 634-642.

Lan, Y. and Jiang, R. (2009). Sonic hedgehog signaling regulates reciprocal epithelial-mesenchymal interactions controlling palatal outgrowth. *Development* **136**, 1387-1396.

Lan, Y., Xu, J. and Jiang, R. (2015). Cellular and molecular mechanisms of palatogenesis. *Curr. Top. Dev. Biol.* **115**, 59-84.

Leslie, E. J., Mancuso, J. L., Schutte, B. C., Cooper, M. E., Durda, K. M., L'Heureux, J., Zucchero, T. M., Marazita, M. L. and Murray, J. C. (2013). Search for genetic modifiers of IRF6 and genotype-phenotype correlations in Van der Woude and popliteal pterygium syndromes. *Am. J. Med. Genet. A* **161**, 2535-2544.

Leslie, E. J., Carlson, J. C., Shaffer, J. R., Feingold, E., Wehby, G., Laurie, C. A., Jain, D., Laurie, C. C., Doheny, K. F., Mchenry, T. et al. (2016a). A multi-ethnic genome-wide association study identifies novel loci for non-syndromic cleft lip with or without cleft palate on 2p24.2, 17q23 and 19q13. *Hum. Mol. Genet.* **25**, 2862-2872.

Leslie, E. J., Koboldt, D. C., Kang, C. J., Ma, L., Hecht, J. T., Wehby, G. L., Christensen, K., Czeizel, A. E., Deleyiannis, F. W.-B., Fulton, R. S. et al. (2016b). IRF6 mutation screening in non-syndromic orofacial clefting: analysis of 1521 families. *Clin. Genet.* **90**, 28-34.

Li, H. and Williams, T. (2013). Separation of mouse embryonic facial ectoderm and mesenchyme. *J. Vis. Exp.* **74**, e50248.

Lidral, A. C., Moreno, L. M. and Bullard, S. A. (2008). Genetic factors and orofacial clefting. *Semin. Orthod.* **14**, 103-114.

Lipinski, R. J., Cook, C. H., Barnett, D. H., Gipp, J. J., Peterson, R. E. and Bushman, W. (2005). Sonic hedgehog signaling regulates the expression of insulin-like growth factor binding protein-6 during fetal prostate development. *Dev. Dyn.* **233**, 829-836.

Lipinski, R. J., Gipp, J. J., Zhang, J., Doles, J. D. and Bushman, W. (2006). Unique and complimentary activities of the Gli transcription factors in Hedgehog signaling. *Exp. Cell Res.* **312**, 1925-1938.

Lipinski, R. J., Bijlsma, M. F., Gipp, J. J., Podhaizer, D. J. and Bushman, W. (2008a). Establishment and characterization of immortalized Gli-null mouse embryonic fibroblast cell lines. *BMC Cell Biol.* **9**, 49.

Lipinski, R. J., Hutson, P. R., Hannam, P. W., Nydza, R. J., Washington, I. M., Moore, R. W., Girdaukas, G. G., Peterson, R. E. and Bushman, W. (2008b). Dose- and route-dependent teratogenicity, toxicity, and pharmacokinetic profiles of the hedgehog signaling antagonist cyclopamine in the mouse. *Toxicol. Sci.* **104**, 189-197.

Lipinski, R. J., Song, C., Sulik, K. K., Everson, J. L., Gipp, J. J., Yan, D., Bushman, W. and Rowland, I. J. (2010). Cleft lip and palate results from Hedgehog signaling antagonism in the mouse: Phenotypic characterization and clinical implications. *Birth Defects Res. A Clin. Mol. Teratol.* **88**, 232-240.

Lipinski, R. J., Holloway, H. T., O'leary-Moore, S. K., Ament, J. J., Pecevich, S. J., Cofer, G. P., Budin, F., Everson, J. L., Johnson, G. A. and Sulik, K. K. (2014). Characterization of subtle brain abnormalities in a mouse model of

hedgehog pathway antagonist-induced cleft lip and palate. *PLoS ONE* **9**, e102603.

Loots, G. G., Ovcharenko, I., Pachter, L., Dubchak, I. and Rubin, E. M. (2002). rVista for comparative sequence-based discovery of functional transcription factor binding sites. *Genome Res.* **12**, 832-839.

Ludwig, K. U., Mangold, E., Herms, S., Nowak, S., Reutter, H., Paul, A., Becker, J., Herberz, R., Alchawa, T., Nasser, E. et al. (2012). Genome-wide meta-analyses of nonsyndromic cleft lip with or without cleft palate identify six new risk loci. *Nat. Genet.* **44**, 968-971.

Ludwig, K. U., Böhmer, A. C., Rubini, M., Mossey, P. A., Herms, S., Nowak, S., Reutter, H., Alblas, M. A., Lippke, B., Barth, S. et al. (2014). Strong association of variants around FOXE1 and orofacial clefting. *J. Dent. Res.* **93**, 376-381.

Madison, B. B., Mckenna, L. B., Dolson, D., Epstein, D. J. and Kaestner, K. H. (2009). FoxF1 and FoxL1 link hedgehog signaling and the control of epithelial proliferation in the developing stomach and intestine. *J. Biol. Chem.* **284**, 5936-5944.

Marcucio, R. S., Cordero, D. R., Hu, D. and Helms, J. A. (2005). Molecular interactions coordinating the development of the forebrain and face. *Dev. Biol.* **284**, 48-61.

Moreno, L. M., Mansilla, M. A., Bullard, S. A., Cooper, M. E., Busch, T. D., Machida, J., Johnson, M. K., Brauer, D., Krahn, K., Daack-Hirsch, S. et al. (2009). FOXE1 association with both isolated cleft lip with or without cleft palate, and isolated cleft palate. *Hum. Mol. Genet.* **18**, 4879-4896.

Murthy, J. and Bhaskar, L. V. K. S. (2009). Current concepts in genetics of nonsyndromic clefts. *Indian J. Plast. Surg.* **42**, 68-81.

Nik, A. M., Johansson, J. A., Ghiami, M., Reyahi, A. and Carlsson, P. (2016). Foxf2 is required for secondary palate development and Tgfβ signaling in palatal shelf mesenchyme. *Dev. Biol.* **415**, 14-23.

Ormestad, M., Astorga, J., Landgren, H., Wang, T., Johansson, B. R., Miura, N. and Carlsson, P. (2006). Foxf1 and Foxf2 control murine gut development by limiting mesenchymal Wnt signaling and promoting extracellular matrix production. *Development* **133**, 833-843.

Rahimov, F., Jugessur, A. and Murray, J. C. (2012). Genetics of nonsyndromic orofacial clefts. *Cleft Palate Craniofac. J.* **49**, 73-91.

Robarge, K. D., Brunton, S. A., Castanedo, G. M., Cui, Y., Dina, M. S., Goldsmith, R., Gould, S. E., Guichert, O., Gunzner, J. L., Halladay, J. et al. (2009). GDC-0449-a potent inhibitor of the hedgehog pathway. *Bioorg. Med. Chem. Lett.* **19**, 5576-5581.

Roessler, E., Ermilov, A. N., Grange, D. K., Wang, A., Grachtchouk, M., Dlugosz, A. A. and Muenke, M. (2005). A previously unidentified amino-terminal domain regulates transcriptional activity of wild-type and disease-associated human GLI2. *Hum. Mol. Genet.* **14**, 2181-2188.

Ruiz i Altaba, A., Prezioso, V. R., Darnell, J. E. and Jessell, T. M. (1993). Sequential expression of HNF-3 beta and HNF-3 alpha by embryonic organizing centers: the dorsal lip/node, notochord and floor plate. *Mech. Dev.* **44**, 91-108.

Sasaki, H. and Hogan, B. L. M. (1994). HNF-3 beta as a regulator of floor plate development. *Cell* **76**, 103-115.

Sasaki, H., Hui, C., Nakafuku, M. and Kondoh, H. (1997). A binding site for Gli proteins is essential for HNF-3beta floor plate enhancer activity in transgenics and can respond to Shh in vitro. *Development* **124**, 1313-1322.

Schenker, N. and Gentleman, J. F. (2001). On judging the significance of differences by examining the overlap between confidence intervals. *Am. Stat.* **55**, 182-186.

Theiler, K. (1989). *The House Mouse: Atlas of Embryonic Development*. New York: Springer.

Wang, T., Tamakoshi, T., Uezato, T., Shu, F., Kanzaki-Kato, N., Fu, Y., Koseki, H., Yoshida, N., Sugiyama, T. and Miura, N. (2003). Forkhead transcription factor Foxf2 (LUN)-deficient mice exhibit abnormal development of secondary palate. *Dev. Biol.* **259**, 83-94.

Watkins, S. E., Meyer, R. E., Strauss, R. P. and Aylsworth, A. S. (2014). Classification, epidemiology, and genetics of orofacial clefts. *Clin. Plast. Surg.* **41**, 149-163.

Xavier, G. M., Seppala, M., Barrell, W., Birjandi, A. A., Geoghegan, F. and Cobourne, M. T. (2016). Hedgehog receptor function during craniofacial development. *Dev. Biol.* **415**, 198-215.

Xie, J., Murone, M., Luoh, S.-M., Ryan, A., Gu, Q., Zhang, C., Bonifas, J. M., Lam, C.-W., Hynes, M., Goddard, A. et al. (1998). Activating Smoothened mutations in sporadic basal-cell carcinoma. *Nature* **391**, 90-92.

Xu, X.-F., Guo, C.-Y., Liu, J., Yang, W.-J., Xia, Y.-J., Xu, L., Yu, Y.-C. and Wang, X.-P. (2009). Gli1 maintains cell survival by up-regulating IGFBP6 and Bcl-2 through promoter regions in parallel manner in pancreatic cancer cells. *J. Carcinog.* **8**, 13.

Xu, J., Liu, H., Lan, Y., Aronow, B. J., Kalinichenko, V. V. and Jiang, R. (2016). A Shh-Foxf-Fgf18-Shh molecular circuit regulating palate development. *PLoS Genet.* **12**, e1005769.

Yoon, J. W., Kita, Y., Frank, D. J., Majewski, R. R., Konicek, B. A., Nobrega, M. A., Jacob, H., Walterhouse, D. and Iannaccone, P. (2002). Gene expression profiling leads to identification of GLI1-binding elements in target genes and a role for multiple downstream pathways in GLI1-induced cell transformation. *J. Biol. Chem.* **277**, 5548-5555.